Published in final edited form as:
Curr Opin Biotechnol. 2009 February ; 20(1): 74–82. doi:10.1016/j.copbio.2009.01.009.

Lymphatic Imaging in Humans with Near-Infrared Fluorescence

John C. Rasmussen[†], **I-Chih Tan**[†], **Milton V. Marshall**[†], **Caroline E. Fife**[§,‡], and **Eva M. Sevick-Muraca**[†,*]

† *Center of Molecular Imaging, Institute of Molecular Medicine, University of Texas Health Science Center at Houston, 1825 Pressler St. SRB 330A, Houston, TX 77030*

§ *Division of Cardiology, Memorial Hermann Hospital, Houston, TX 77030*

‡ *Center for Wound Healing and Lymphedema Therapy, Memorial Hermann Hospital, Houston, TX 77030*

Summary

While the lymphatic system is increasingly associated with diseases of prevalence, study of these diseases is difficult owing to the paucity of imaging techniques with the sensitivity and temporal resolution to discriminate lymphatic function. Herein, we review the known, pertinent features of the human lymphatic system in health and disease and set the context for a number of emerging studies that use near-infrared fluorescence imaging to non-invasively assess tumor draining lymphatic basins in cancer patients, intraoperatively guide resection of first draining lymph nodes, and to interrogate the difference between normal and aberrant lymphatic structure and function.

Introduction

Besides the advantages for interrogating subcellular, cellular, and tissue length scales, fluorescent labeling offers exquisite sensitivity that over the past decades, has enabled it to supplant many radiotracers in several laboratory procedures. Yet in medical imaging, nuclear imaging procedures with planar gamma imaging, single photon emission computed tomography, or positron emission tomography continue to be the “gold-standard” of non-invasive molecular imaging in both preclinical and clinical studies. Unlike the high energy photons associated with nuclear imaging procedures, low energy photons associated with fluorescence imaging suffer significant attenuation caused by tissue absorption and scattering properties, as well as significant levels of autofluorescence at excitation wavelengths below 750 nm that lead to high background levels. Near-infrared (NIR) fluorescence imaging (caused by excitation > 750 nm) may have the advantages of little or no autofluorescence as well as significant tissue penetration depths that permit repeated activation of NIR excitable fluorophores and multiple radiative relaxation events. The results may be increased photon count rates in comparison to radiotracers, whose one-time relaxation cause single photon events for collection and image registration. To date, the opportunities and limitations of NIR fluorescence imaging for non-invasive medical imaging have begun to be investigated in the lymphatic system where nuclear imaging techniques of scintigraphy and radioimmunoscintigraphy have remained “gold-standard” imaging techniques. In the following, we briefly provide a background of the lymphatic system, review nuclear imaging

*Corresponding author: Eva M. Sevick-Muraca, Telephone: 713-500-3560, Fax: 713-500-0319, E-mail: eva.sevick@uth.tmc.edu.

techniques associated with its imaging, and then describe NIR fluorescence imaging studies to interrogate human lymphatic architecture and function in disease and health.

Background: The Lymphatic System

Despite being termed "the forgotten circulation," [1•] the lymphatic system is responsible for fluid homeostasis, mediating immune response, and lipid absorption.[2•] The lymphatic system has been implicated in several diseases of increasing prevalence, such as asthma, obesity, diabetes, and cancer metastasis. ([3–5], for review see [1•,2•]) However our understanding of the lymphatic system has been severely limited by the lack of *in vivo* lymphatic imaging techniques due in part to the limited contrast of lymphatic fluids and structures. The normal lymphatic system is unidirectional and begins with the uptake of interstitial fluids via the lymph plexus in the intradermal space or lymphatic capillaries that line key structures throughout the body. From the plexus, lymph travels through lymphatic vessels via the action of contractile lymphangions to the lymph nodes where transported particles are taken up by antigen presenting cells for immune presentation and stimulation. From the lymph nodes, the lymph is propelled to the subclavian vein for entry into the blood circulatory system. Lymphangions are vessel subunits bounded by valves that prevent backflow, propel lymph forward, and ensure unidirectional flow in healthy lymphatics.

Failure of the lymphatic system typically results in a condition known as lymphedema and is characterized by chronic swelling, tissue fibrosis, and susceptibility to infection. The fundamental causes of lymphatic failure are not well understood, but can stem from genetic causes, as in the case of lymphedema-distichiasis (LD) syndrome in which a mutation in the forkhead transcription factor FOXC2 causes the lymphatic valves to malfunction resulting in poor lymphatic flow. In the Western world, lymphedema is predominately acquired and occurs days or years after an initial trauma to the lymphatics, such as lymph node resection or surgery. The exact etiology of acquired lymphedema remains unknown. In the developing world, the filarial parasite is responsible for a form of acquired lymphedema commonly called elephantitis. Regardless of whether congenital or acquired, there is no known cure for lymphedema, and treatment is typically limited to a regimen of massage and compression bandaging to control edema. Perhaps the single largest contributing factor preventing the development of new treatment options has been the lack of techniques for imaging real time dynamic lymph flow to discern lymphatic function.

Lymphography and lymphoscintigraphy

Until recently, only two imaging techniques have been available to directly image the lymphatics, lymphangiography and lymphoscintigraphy as detailed in a recent review [6]. Briefly, over a half a century old, lymphangiography involves the cannulation of lymphatic vessels for administration of milliliter volumes of CT or MR contrast agents. Unfortunately, the technical skill required for lymph vessel cannulation and complications from contrast agents prevent the widespread use of lymphangiography. Lymphoscintigraphy is currently the "gold-standard" imaging technique to assess lymph drainage and consists of intradermal or intraparenchymal injections of filtered ^{99m}Technetium sulfur colloid (40–100 nm in diameter) or ^{99m} Technetium albumin nanocolloid (5–80 nm in diameter) for direct uptake into the lymphatic plexus and, for planar gamma scintigraphy, to map the regional lymph system. Images are typically acquired over several minutes to identify the first tumor draining LNs (i.e., the "sentinel" LN) and to visualize major trunks of the lymphatic system. Lymphoscintigraphy is also used to diagnose blockages of the lymph system that result in lymphedema. [7,8] Similar to lymphoscintigraphy and under development for over a decade, radioimmunoscintigraphy employs radiolabeled antibodies that target cancer epitope in the

hope of imaging cancer-positive lymph nodes ([9], for review see [10]). Images are typically integrated over several minutes in order to achieve images for sufficient target-to-background.

Dynamic lymphoscintigraphy captures the advancing front of radiocolloid from the injection site through the lymphatics using a series of gamma images that are acquired with exposure or integration times as short as 20 seconds. The technique has been reported to discriminate sentinel LNs and those that are secondary or drain the sentinel LN. [11–14] Using dynamic lymphoscintigraphy, Uren and colleagues reported the movement of radiocolloids through the lymphatic vessels at velocities ranging from 1.5 cm/min in the head and neck to 10.2 cm/min in the leg and foot. [13] However, the finite particle size and the comparatively long integration times prevent direct imaging of contractile lymph flow.

Near-infrared fluorescent optical imaging

NIR fluorescence imaging has the opportunity to provide more rapid imaging of lymphatic function owing to the increased sensitivity associated with higher photon count rates from NIR organic fluorophores over radiotracers. First demonstrated in animal models such as mice [15,16], rats [17], canines [18••] [19•], and swine [6,20–22] [23••], NIR fluorescent imaging has recently been translated to the clinic for lymph mapping [24] [25•] [26••] [27] [28•] [29], intraoperative guidance [28•] [30,31], and real-time functional imaging [6] [26••] [32•]. Table 1 provides a synopsis of the literature using exogenous indocyanine green (ICG) in off-label studies to image the lymphatic system in humans. ICG is a tricarbocyanine dye that is approved for use for hepatic and ophthalmology applications and is generally administered in adults at a total dose less than 25 mg. Besides its dark green color at 0.5% volume, ICG solutions can be excited between 760 – 785 nm and fluorescence imaged between 820 and 840 nm.

Lymphatic Mapping and Intraoperative Guidance

The use of fluorescent lymphatic imaging in the clinic was first reported in Japan by Kitai *et al.* for mapping and intraoperative identification of sentinel lymph nodes in eighteen breast cancer patients. [28••] In this study, 25mg of indocyanine green (ICG) in 5ml were injected near the areola of eighteen breast cancer patients to visualize the draining subcutaneous lymphatics and identify the sentinel nodes. In similar studies, Tagaya *et al.* identified and resected draining lymph nodes from twenty-five patients after injecting 1mg of ICG near the areola [30] and Fujiwara *et al.* identified and resected sentinel lymph nodes after an unspecified number of injections of 0.5 mg of ICG each near the tumor site in 10 skin cancer patients [29]. Ogata *et al.* used fluorescence from a 1 mg dose of ICG for intraoperative guidance during lymphaticovenular anastomoses.[31] Ogasawara *et al.* used a 25 mg dose of ICG to evaluate lymphatic drainage pathways from different regions of the breast in breast cancer patients. [27] No observations of active propulsion or contractile lymph flow were reported in these studies and these studies suggest that high concentrations of ICG can replace the ~0.1 wt% blue dye solution conventionally used by surgeons to visualize lymph trafficking intraoperatively. The presumed intraoperative advantage to using a NIR excitable fluorescent dye over a blue dye may be in the ability detect subsurface lymphatic structures which may not be readily apparent from direct visual observation of the blue dye.

In a recent study reported by Sevick-Muraca *et al.* non-invasive SLN mapping in 24 breast cancer patients was performed after administration of *microdose* amounts of ICG.[26••] In this dose escalation study subjects were injected with a total of 0.31 to 100 μg of ICG (divided into four injections of 0.1 ml each) around the areola and images were captured using a custom built, intensified, charge coupled device (CCD) NIR optical imager with a typical exposure time of 200 msec. For eight of nine subjects receiving 10μg or more of ICG, draining lymphatic vessels were identified between the areola and the axillary nodal basin. In seven of these eight subjects, distinct packets of lymph were observed transiting the lymphatic vessels with average

apparent velocities ranging from 0.08 to 0.32 cm/sec with an average of 14 to 92 seconds elapsing between propulsion events. No lymphatic structure or function was visible *in vivo* when the total dose of ICG was less than 10μg.

Non-invasive, Functional Lymph Imaging

Others have also determined apparent lymphatic velocities and aberrant lymphatic architectures from NIR fluorescence albeit with high doses of ICG. Unno *et al.* imaged and compared the lymphatic structure of 10 normal subjects and 12 subjects with secondary lymphedema in the legs. [25•] They identified several characteristics of fluorescent images in lymphedema subjects including dermal backflow, dilated lymph vessels with proximal obliteration, and diffuse glittering patches of ICG they called Milky Way signs. Lymphoscintigraphy was also performed and compared favorably with the fluorescent images. In another study, Unno *et al.* performed quantitative lymph imaging to measure transit times from the injection site in the foot to the knee and subsequently to the groin on ten normal subjects. [24] Transit times between injection site and draining LN basins were measured for each subject in each of four positions including standing, lying down, standing with massage, and while performing cycle ergometer exercises; transit times ranged from 53.9 ± 16.2 and 60.3 ± 34.9 seconds in the right and left legs respectively while standing with massage to 357 ± 289 and 653 ± 564 seconds in the right and left legs respectively while standing. In another 17 subjects, fluorescent imaging and dynamic lymphoscintigraphy was performed and a strong correlation of transit times measured by the two methods was found.

We recently completed the imaging portion of a clinical study conducted under an Investigational New Drug (IND) application in which propulsive lymph flow was imaged following off-label, microdose intradermal administration of ICG in the arms or legs of 24 normal subjects and 20 subjects diagnosed with stage I or II lymphedema. [6] [32•] In this study, multiple 0.1 ml intradermal injections of 0.25μg ICG were given in each limb. Typically subjects undergoing hand/arm imaging received four injections (100μg total dose per limb) in the interdigital space or six injections (two on the back of the hand, two just above the outer wrist, and two just above the inner wrist for a total dose of 150μg/limb) on each limb. Subjects undergoing foot/leg imaging typically received eight injections (two on top of foot, one on the heel, two near the ankle, two on the calf, and one on the inner thigh for a total dose of 200μg/limb) on each limb. Immediately after administration, lymphatic trafficking of lymph fluid "packets" from the sites of injection toward the regional nodal basin was observed in all normal subjects and the asymptomatic limbs of lymphedema subjects using a custom intensified CCD camera system with a camera integration time of 200 ms. No adverse events were reported, and skin color did not impact the ability to obtain dynamic lymph images.

Typical NIR fluorescence images representing the lymphatics of typical normal subjects are shown Figure 1a–d. Figure 1a shows the lymphatic structure in the back of the hand of a 22 year old male following the interdigital injections. The brighter localized sections of the lymphatic vasculature are hypothesized to be lymphangions where propelled fluorescent dye frequently accumulates before being released to the next localized region for propulsion up the arm to the axilla. Figure 1b shows the dense lymphatic structure of the arm of a 37 year old male, and online Supplemental Movie #1 illustrates lymphatic propulsion of dye in the form of "packets" from the injection sites to nodes in the axilla. Online Supplemental Movie #2 provides another example of lymphatic propulsion in the arm of a 41 year old female. Figures 1c and 1d show the typical normal lymphatic structure in the foot and lower legs of a 40 year old female, with the online Supplemental Movie #3 illustrating propulsion of ICG from the feet and ankles to the shin. At the shin the "packet" of dye splits, draining into a couple of branches of the lymphatics that conduct the dye up to the knee. Figure 2 illustrates the movement of a packet of lymph, designated by the red oval, along the ventromedial bundle in

the calf of a normal 40 year old female subject (see online Supplemental Movie #4). The outline of the limbs in the Figures and Movies is made possible by the excitation light leakage through the filters [32] which enables automatic registration of the fluorescent signals with the field of view.

Figure 3 further illustrates the pulsatile nature of lymph flow as the detected intensity of selected regions of interest (Figure 3a) is plotted as a function of time (Figure 3b). The first region of interest (ROI 1) includes an area of the foot of a 59 year old female where a lymphangion was thought to be located due to localized pooling of ICG. ROI 2 is located downstream from ROI 1 and was specifically selected as it appeared to be outside of a pooling region. As shown in Figure 3b, the intensity of ROI 1 slowly increases as lymph pools in the lymphangion, when a propulsion event occurs and the lymph rapidly leaves the ROI. Because ROI 2 was presumably chosen to be between lymphangions, its average intensity peaks immediately after the propulsion event and tapers off as the packet transits the region to the next lymphangion. The dynamic behavior of lymphatic function mimics that seen in mice [16].

As also reported by Unno *et al.* [25••] distinct differences between the structure and function of diseased and normal lymphatics were also observed in our microdosing studies. Figure 4 illustrates several typical traits seen in many of the lymphedema subjects, including dermal backflow and the Milky Way sign (Figure 4a) on the arm of a 66 year old female. Dermal backflow was observed to some extent in every diseased limb imaged. Figure 4b illustrates hyperplastic lymphatic growth producing dense, unorganized lymphatic networks in a 57 year old female, Figure 4c illustrates retrograde flow in a 46 year old female, and Figure 4d illustrates tortuous vessels observed in a 48 year old female. Figure 5 illustrates a case in which active back flow was observed in a 48 year old female. In this case, as a packet of lymph is propelled through the lymph vessel, a portion of the packet (enclosed in the red circle) drains back into the propelling lymphangion (see online Supplemental Movie #5 for visualization).

After image acquisition, image sequences are analyzed to determine the apparent velocity of each packet of lymph and the time delay between propulsion events. [23••] To date, quantitative lymph flow data is currently only available for 21 subjects (9 normal and 12 lymphedema). Of these, the apparent velocity in the arms of normal subjects range from 0.13 to 1.72 cm/sec with 7.0 to 250.5 seconds between propulsion events. The apparent velocity in the asymptomatic and symptomatic arms of lymphedema subjects range from 0.06 to 4.89 cm/sec and 0.09 to 3.107 cm/sec with 2.8 to 200.5 seconds and 5.0 to 113.0 seconds between propulsion events respectively. For the legs of normal subjects, the apparent packet velocities ranged from 0.05 to 11.79 cm/sec with 1.5 to 193.8 seconds between propulsion events while the apparent velocities in the asymptomatic and symptomatic legs of lymphedema subjects were 0.20 to 1.45 cm/sec and 0.14 to 2.28 cm/sec with 20.7 to 146.3 seconds and 18.6 to 252.5 seconds between propulsion events respectively. These velocities are significantly faster than those measured using lymphoscintigraphy, and are most likely due to soluble ICG administered at microdose levels as compared to the 99mTc sulfur colloid particles. The soluble dye presumably enables measurement of a packet of lymph fluid rather than the transit of a particle within the lymphatic system.

Future NIR Imaging

Although ICG has successfully been used to image the lymphatics, it possesses limitations such as a low quantum efficiency (0.016), which may limit the signal strength for deep interrogation of tissues and future tomography applications [33–36]. In addition, ICG has no functional group to allow conjugation to targeting moieties that may enable non-invasive nodal staging as sought in radioimmunoscintigraphy. For the full potential of NIR imaging to be

realized, new NIR emitting dyes that possess higher quantum efficiencies and functional groups for conjugation need to be developed and approved for human use.

Dual labeled dyes containing both a radionuclide and a NIR fluorophore have been developed that provide the ability to acquire both fluorescent images and radioscintigrams from the same imaging agent. [37–39][39••] The dual nature of these dyes may prove useful to validate NIR optical imaging against the 'gold standard' scintigraphy, to perform longitudinal studies in which study times exceed the physical half life of the radionuclide, and to provide an alternative to NIR fluorescence for collecting signals that may be too deep for fluorescent imaging.

Conclusions

In the past few years, NIR fluorescent imaging has made significant advances into the clinic with several clinical trials being done to test the feasibility and efficacy of NIR fluorescent imaging of the lymphatic system. Preliminary studies indicate that fluorescent imaging can aid in the identification and surgical resection of sentinel lymph nodes, the diagnosis of lymphedema, and as a tool to visualize and quantitate *in vivo* lymphatic function. As new dyes become available and instrumentation is further developed, NIR fluorescent imaging may play a significant role in furthering our understanding of the lymphatic system and its role in the health of the body. The ability to collect fluorescent signals in humans following microdose administration of ICG (an inefficient, non-specific NIR fluorophore) is consistent with the increased photon count rates expected from the repeated radiative relaxations. The enhanced sensitivity bodes well for the translation of brighter NIR fluorophores with functional groups.

Supplementary Material

Refer to Web version on PubMed Central for supplementary material.

Acknowledgments

We would like to acknowledge Kristen E. Adams, Ruchi Sharma, Erik A. Maus, Latisha A. Smith, Juliet A. Wendt, Glenn Wilson, and Nallely Connoly for their clinical assistance. This work is supported in parts by the National Institutes of Health (R01 CA112679) and the Longaberger Foundation through the American Cancer Society Research Scholar Grant (RSG-06-213-01-LR).

Abbreviations

CCD
: charge coupled device

CT
: x-ray computed tomography

FOXC2
: forkhead transcription factor

ICG
: indocyanine green

LD
: lymphedema-distichiasis

LN
: lymph node

MR

magnetic resonance imaging

NIR

near-infrared

ROI

region of interest

SLN

sentinel lymph node

References and Recommended Reading

1. Rockson, SG. The lymphatic continuum revisited. Boston, Mass.: Published by Blackwell Pub. on behalf of the New York Academy of Sciences; 2008. • Excellent compendium of lymphatic disorders and molecular mechanisms;
2•. Alitalo K, Tammela T, Petrova TV. Lymphangiogenesis in development and human disease. Nature 2005;438:946–953. [PubMed: 16355212]Excellent review of molecular signaling in lymphangiogenesis.
3. Baluk P, Tammela T, Ator E, Lyubynska N, Achen MG, Hicklin DJ, Jeltsch M, Petrova TV, Pytowski B, Stacker SA, et al. Pathogenesis of persistent lymphatic vessel hyperplasia in chronic airway inflammation. J Clin Invest 2005;115:247–257. [PubMed: 15668734]
4. Harvey NL, Srinivasan RS, Dillard ME, Johnson NC, Witte MH, Boyd K, Sleeman MW, Oliver G. Lymphatic vascular defects promoted by Prox1 haploinsufficiency cause adult-onset obesity. Nat Genet 2005;37:1072–1081. [PubMed: 16170315]
5. Ji RC. Characteristics of lymphatic endothelial cells in physiological and pathological conditions. Histol Histopathol 2005;20:155–175. [PubMed: 15578435]
6. Sharma R, Wendt JA, Rasmussen JC, Adams KE, Marshall MV, Sevick-Muraca EM. New horizons for imaging lymphatic function. Ann N Y Acad Sci 2008;1131:13–36. [PubMed: 18519956]
7. McNeill GC, Witte MH, Witte CL, Williams WH, Hall JN, Patton DD, Pond GD, Woolfenden JM. Whole-body lymphangioscintigraphy: preferred method for initial assessment of the peripheral lymphatic system. Radiology 1989;172:495–502. [PubMed: 2748831]
8. Yuan Z, Chen L, Luo Q, Zhu J, Lu H, Zhu R. The role of radionuclide lymphoscintigraphy in extremity lymphedema. Ann Nucl Med 2006;20:341–344. [PubMed: 16878705]
9. Weinstein JN, Steller MA, Keenan AM, Covell DG, Key ME, Sieber SM, Oldham RK, Hwang KM, Parker RJ. Monoclonal antibodies in the lymphatics: selective delivery to lymph node metastases of a solid tumor. Science 1983;222:423–426. [PubMed: 6623082]
10. Sampath L, Wang W, Sevick-Muraca EM. Near infrared fluorescent optical imaging for nodal staging. Journal of Biomedical Optics 2008;13:041312. [PubMed: 19021320]
11. Lee AC, Keshtgar MR, Waddington WA, Ell PJ. The role of dynamic imaging in sentinel lymph node biopsy in breast cancer. Eur J Cancer 2002;38:784–787. [PubMed: 11937312]
12. Mariani G, Gipponi M, Moresco L, Villa G, Bartolomei M, Mazzarol G, Bagnara MC, Romanini A, Cafiero F, Paganelli G, et al. Radioguided sentinel lymph node biopsy in malignant cutaneous melanoma. J Nucl Med 2002;43:811–827. [PubMed: 12050328]
13. Uren RF, Howman-Giles R, Thompson JF. Patterns of lymphatic drainage from the skin in patients with melanoma. Journal of Nuclear Medicine 2003;44:570–582. [PubMed: 12679402]
14. Uren RF. Lymphatic drainage of the skin. Annals of Surgical Oncology 2004;11:179s–185s. [PubMed: 15023748]
15. Wunderbaldinger P. Optical imaging of lymph nodes. European Journal of Radiology 2006;58:390–393. [PubMed: 16473488]
16. Kwon S, Sevick-Muraca EM. Noninvasive quantitative imaging of lymph function in mice. Lymphat Res Biol 2007;5:219–231. [PubMed: 18370912]
17. Ogata F, Azuma R, Kikuchi M, Koshima I, Morimoto Y. Novel lymphography using indocyanine green dye for near-infrared fluorescence labeling. Annals of Plastic Surgery 2007;58:652–655. [PubMed: 17522489]

18••. Reynolds JS, Troy TL, Mayer RH, Thompson AB, Waters DJ, Cornell KK, Snyder PW, Sevick-Muraca EM. Imaging of spontaneous canine mammary tumors using fluorescent contrast agents. Photochem Photobiol 1999;70:87–94. [PubMed: 10420847]First proposal of fluorescent optical imaging of lymph nodes.

19•. Gurfinkel M, Thompson AB, Ralston W, Troy TL, Moore AL, Moore TA, Gust JD, Tatman D, Reynolds JS, Muggenburg B, et al. Pharmacokinetics of ICG and HPPH-car for the detection of normal and tumor tissue using fluorescence, near-infrared reflectance imaging: a case study. Photochem Photobiol 2000;72:94–102. [PubMed: 10911733]First dynamical imaging of the lymphatic system in animals.

20. Tanaka E, Choi HS, Fujii H, Bawendi MG, Frangioni JV. Image-guided oncologic surgery using invisible light: completed pre-clinical development for sentinel lymph node mapping. Ann Surg Oncol 2006;13:1671–1681. [PubMed: 17009138]

21. Soltesz EG, Kim S, Kim SW, Laurence RG, De Grand AM, Parungo CP, Cohn LH, Bawendi MG, Frangioni JV. Sentinel lymph node mapping of the gastrointestinal tract by using invisible light. Ann Surg Oncol 2006;13:386–396. [PubMed: 16485157]

22. Parungo CP, Ohnishi S, Kim SW, Kim S, Laurence RG, Soltesz EG, Chen FY, Colson YL, Cohn LH, Bawendi MG, et al. Intraoperative identification of esophageal sentinel lymph nodes with near-infrared fluorescence imaging. J Thorac Cardiovasc Surg 2005;129:844–850. [PubMed: 15821653]

23••. Sharma R, Wang W, Rasmussen JC, Joshi A, Houston JP, Adams KE, Cameron A, Ke S, Kwon S, Mawad ME, et al. Quantitative imaging of lymph function. Am J Physiol Heart Circ Physiol 2007;292:H3109–3118. [PubMed: 17307997]First documented report of propulsive lymph flow in animals using NIR fluorescence imaging.

24. Unno N, Nishiyama M, Suzuki M, Yamamoto N, Inuzuka K, Sagara D, Tanaka H, Konno H. Quantitative lymph imaging for assessment of lymph function using indocyanine green fluorescence lymphography. Eur J Vasc Endovasc Surg 2008;36:230–236. [PubMed: 18534875]

25•. Unno N, Inuzuka K, Suzuki M, Yamamoto N, Sagara D, Nishiyama M, Konno H. Preliminary experience with a novel fluorescence lymphography using indocyanine green in patients with secondary lymphedema. J Vasc Surg 2007;45:1016–1021. [PubMed: 17391894]First report of NIR fluorescence imaging of diseased lymphatics.

26••. Sevick-Muraca EM, Sharma R, Rasmussen JC, Marshall MV, Wendt JA, Pham HQ, Bonefas E, Houston JP, Sampath L, Adams KE, et al. Imaging of lymph flow in breast cancer patients after microdose administration of a near-infrared fluorophore: feasibility study. Radiology 2008;246:734–741. [PubMed: 18223125]First report of NIR fluorescent imaging in humans with microdose amounts of contrast agent.

27. Ogasawara Y, Ikeda H, Takahashi M, Kawasaki K, Doihara H. Evaluation of breast lymphatic pathways with indocyanine green fluorescence imaging in patients with breast cancer. World J Surg 2008;32:1924–1929. [PubMed: 18330628]

28•. Kitai T, Inomoto T, Miwa M, Shikayama T. Fluorescence navigation with indocyanine green for detecting sentinel lymph nodes in breast cancer. Breast Cancer 2005;12:211–215. [PubMed: 16110291]First use of NIR fluorescence in humans for lymphatic imaging.

29. Fujiwara M, Mizukami T, Suzuki A, Fukamizu H. Sentinel lymph node detection in skin cancer patients using real-time fluorescence navigation with indocyanine green: preliminary experience. J Plast Reconstr Aesthet Surg. 2008

30. Tagaya N, Yamazaki R, Nakagawa A, Abe A, Hamada K, Kubota K, Oyama T. Intraoperative identification of sentinel lymph nodes by near-infrared fluorescence imaging in patients with breast cancer. American Journal of Surgery 2008;195:850–853. [PubMed: 18353274]

31. Ogata F, Narushima M, Mihara M, Azuma R, Morimoto Y, Koshima I. Intraoperative lymphography using indocyanine green dye for near-infrared fluorescence labeling in lymphedema. Annals of Plastic Surgery 2007;59:180–184. [PubMed: 17667413]

32•. Sevick-Muraca EM, Rasmussen JC. Molecular imaging with optics: primer and case for near-infrared fluorescence techniques in personalized medicine. Journal of Biomedical Optics 2008;13:041303. [PubMed: 19021311]Treatise on physics and instrumentation of NIR fluorescence imaging.

33. Ntziachristos V, Bremer C, Weissleder R. Fluorescence imaging with near-infrared light: new technological advances that enable in vivo molecular imaging. European Radiology 2003;13:195–208. [PubMed: 12541130]

34. Godavarty A, Sevick-Muraca EM, Eppstein MJ. Three-dimensional fluorescence lifetime tomography. Med Phys 2005;32:992–1000. [PubMed: 15895582]

35. Liang XP, Zhang QZ, Li CQ, Grobmyer SR, Fajardo LL, Jiang HB. Phase-contrast diffuse optical tomography: Pilot results in the breast. Academic Radiology 2008;15:859–866. [PubMed: 18572121]

36. Ge J, Zhu B, Regalado S, Godavarty A. Three-dimensional fluorescence-enhanced optical tomography using a hand-held probe based imaging system. Med Phys 2008;35:3354–3363. [PubMed: 18697559]

37. Li C, Wang W, Wu Q, Ke S, Houston J, Sevick-Muraca E, Dong L, Chow D, Charnsangavej C, Gelovani JG. Dual optical and nuclear imaging in human melanoma xenografts using a single targeted imaging probe. Nucl Med Biol 2006;33:349–358. [PubMed: 16631083]

38. Sampath L, Kwon S, Ke S, Wang W, Schiff R, Mawad ME, Sevick-Muraca EM. Dual-labeled trastuzumab-based imaging agent for the detection of human epidermal growth factor receptor 2 overexpression in breast cancer. J Nucl Med 2007;48:1501–1510. [PubMed: 17785729]

39••. Houston JP, Ke S, Wang W, Li C, Sevick-Muraca EM. Quality analysis of in vivo near-infrared fluorescence and conventional gamma images acquired using a dual-labeled tumor-targeting probe. J Biomed Opt 2005;10:054010. [PubMed: 16292970]First comparative assessment of nuclear and optical probes.

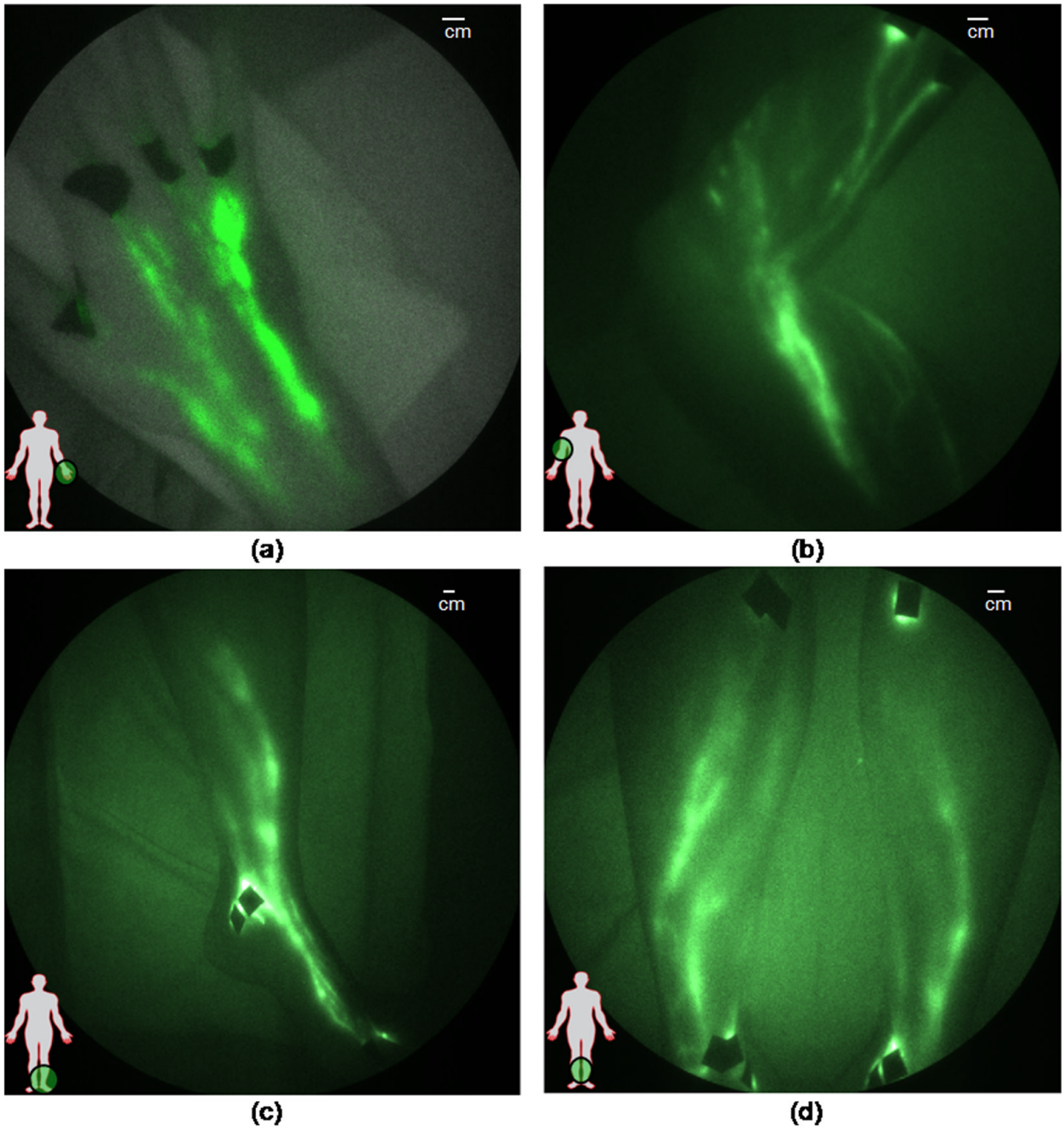

Figure 1.
Images of healthy lymphatics typically seen in normal subjects. Lymphatic vessels in (a) hand (adapted from Sharma, *et al.* [6]), (b) arm with hand above the head (see Supplemental Movie #1 and Supplemental Movie #2), (c) foot, ankle, and leg, and (d) both lower legs (adapted from Sevick-Muraca and Rasmussen [32•], see also Supplemental Movie #3). Black spots are covered injection sites.

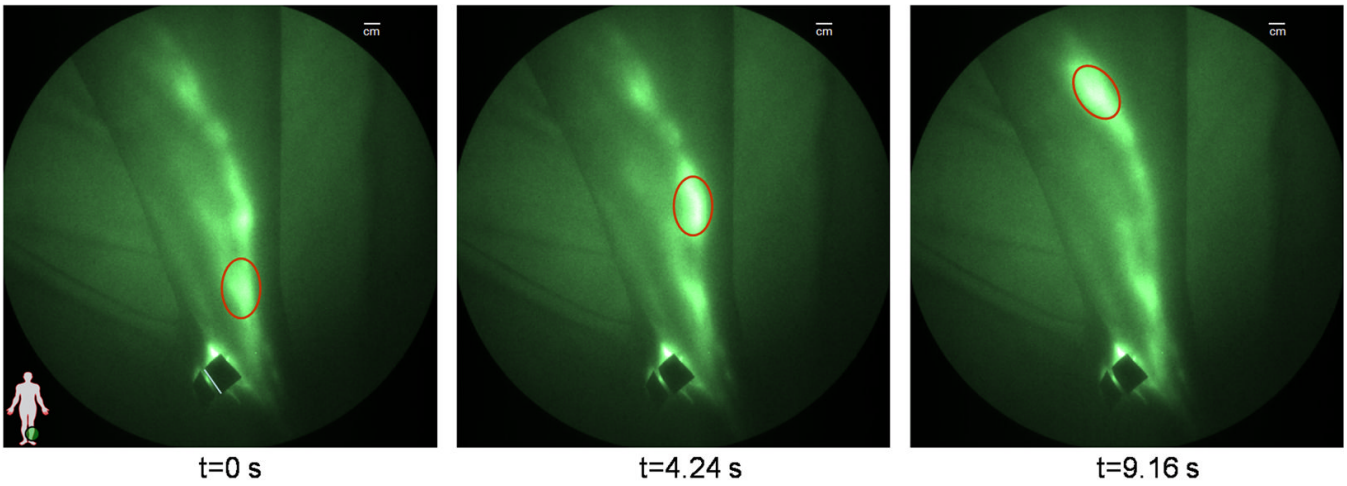

Figure 2.
The movement of a packet of lymph (red oval) as it is propelled up a lymphatic vessel in a normal leg (see Supplemental Movie #4). Black spots are covered injection sites.

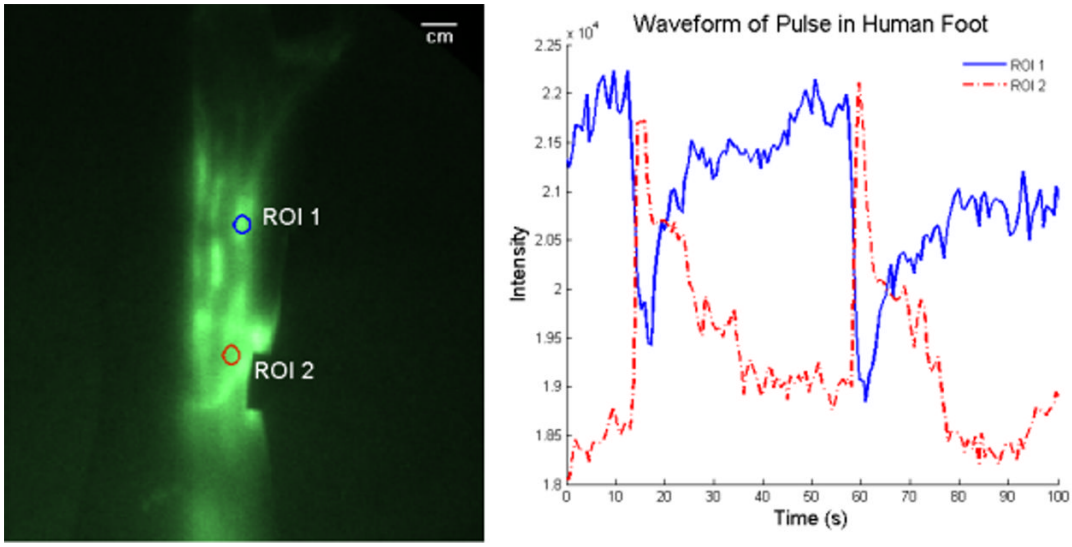

Figure 3.

Illustration of the intensity profile and hence the ICG concentration in different parts of the lymphatic vessel. ROI 1 illustrates the rise in fluorescent intensity as the ICG collects in a lymphangion of the foot. When the lymphangion is filled, it contracts and sends the ICG through the vessel. ROI 2 illustrates the fluorescence intensity as a packet of lymph flows through a non-lymphangion region. Black spot is covered injection site.

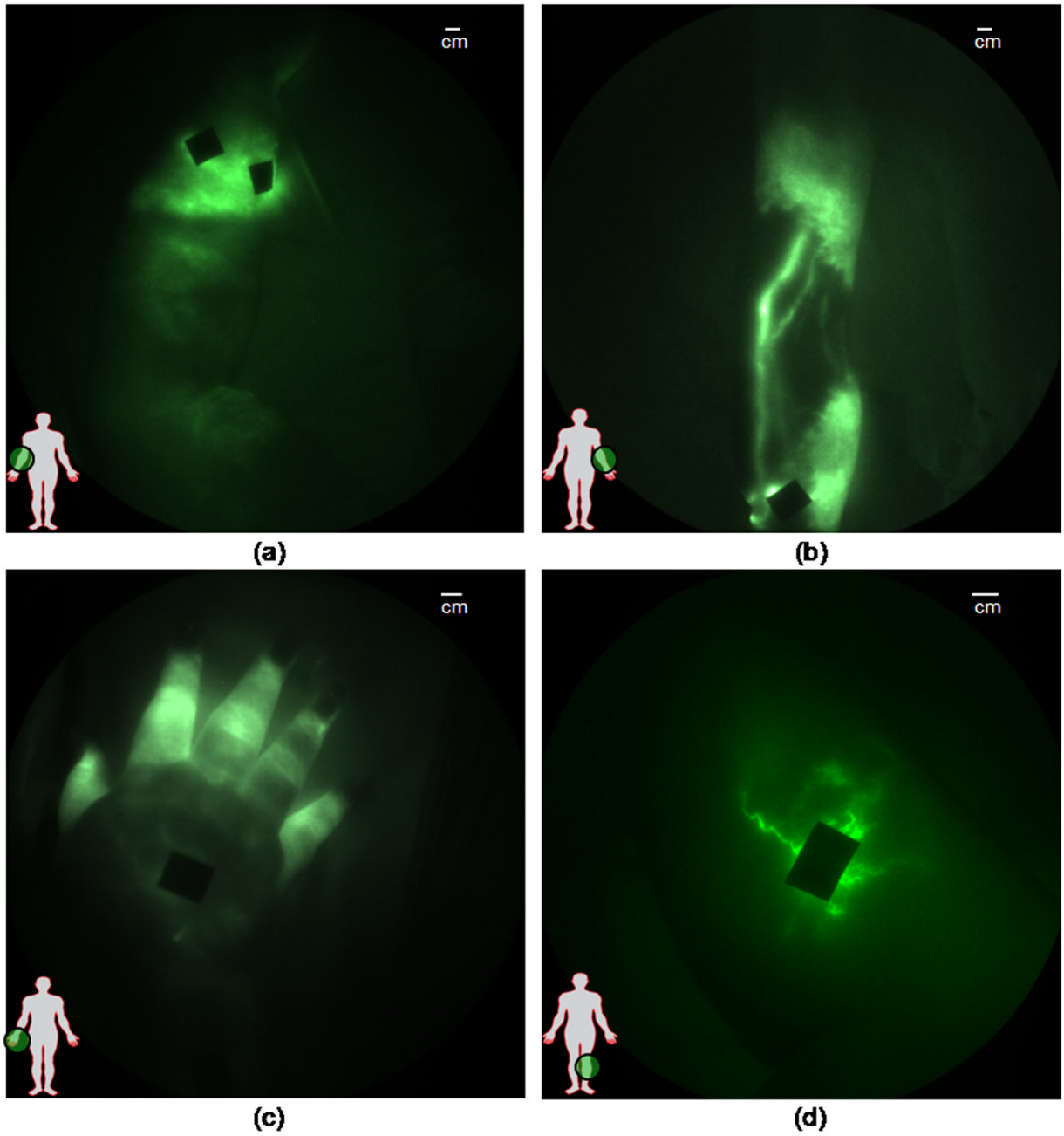

Figure 4.
Images of diseased lymphatics, (a) diffused dye patterns in symptomatic arm, (b) hyperplastic growth in symptomatic arm, (c) retrograde flow in symptomatic hand, and (d) tortuous vessels in symptomatic leg. Black spots are covered injection sites.

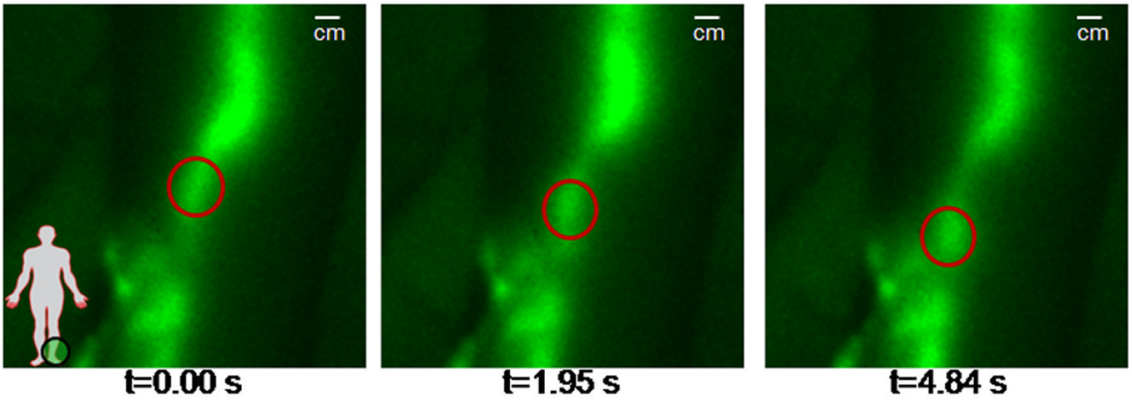

Figure 5.
The retrograde movement of a packet of lymph (red circle) in a symptomatic leg with apparent valvular insufficiency (See Supplemental Movie #5). Black spot is covered injection site.

Table 1

Review of fluorescence imaging of the lymphatics.

Author, Year, [ref]	# of Subjects	Study Aim	Dosage	Comments
Kitai *et al.*, 2005,[28•]	18	Sentinel lymph node mapping and resection in breast cancer patients.	Unspecified amount of 5mg/ml ICG	Observed subcutaneous lymphatic vessels in all patients and identified sentinel nodes in 17 patients. No active propulsion reported.
Ogata *et al.*, 2007, [31]	5	Intraoperative guidance for persons with lymphedema.	1 mg ICG	Used fluorescence imaging to intraoperatively guide lymphaticovenular anastomoses for treatment of lymphedema.
Unno *et al.*, 2007, [25•]	22	Diagnose lymphedema using fluorescence imaging.	1 mg ICG	Imaged and compared the lymphatics of 10 normal subjects and 12 subjects with secondary lymphedema of the leg. Identified characteristic fluorescent features in lymphedema subjects and compared to lymphoscintigraphy.
Fujiwara *et al.*, 2008, [29]	10	Sentinel lymph node mapping and resection in skin cancer patients.	Unspecified number of injections containing 0.5 mg ICG	Successfully observed and identified lymphatic vessels and sentinel nodes in all subjects. No active propulsion was reported.
Sevick-Muraca *et al.*, 2008, [26••]	24	Dose escalation study for sentinel lymph node mapping in breast cancer patients.	0.31–100 μg ICG	Established minimal dosage of ICG needed to observe lymphatic trafficking to sentinel nodes. To our knowledge is the first time active lymphatic propulsion was observed in humans.
Ogasawara *et al.*, 2008, [27]	37	Evaluate breast lymphatic pathways in patients with breast cancer.	25 mg ICG	Monitored lymph drainage pathways from different areas of the breast to the axilla.
Unno *et al.*, 2008, [24]	27	Measure transit times of dye from injection to knees and inguinal region.	1.5 mg ICG	Imaged and compared transit times to knee and groin of 10 normal subjects and 17 subjects undergoing abdominal aortic aneurysm treatment. Correlated fluorescent velocities with lymphoscintigraphy velocities. Reported pulsatile flow in one lymphatic vessel.
Sevick-Muraca and Rasmussen, 2008, [32•] Sharma *et al.*, 2008, [6]	44	An ongoing study to quantitatively compare lymph function between normal and lymphedema subjects.	100–400 μg ICG	These papers provided snapshots of an ongoing clinical trial of lymphatic function. Velocity and period of propulsive flow were calculated, and the structure of normal and diseased lymphatics investigated.